Journal of Structural Geology, Vol 13, No 7, pp 743 to 758, 1991
Printed in Great Britain

0191-8141/91 $03 00+0 00

Partitioning of transpressive motions within a sigmoidal foldbelt: the Variscan Sierras Australes, Argentina

P. R. COBBOLD and D. GAPAIS

Centre Armoricain d'Etude Structurale des Socles (CNRS), Université de Rennes, 35042 Rennes Cédex, France

and

E. A. ROSSELLO

CONICET and Departamento de Ciencias Geológicas, Universidad de Buenos Aires, Ciudad Universitaria, 1428 Buenos Aires, Argentina

(*Received* 24 *July* 1990; *accepted in revised form* 11 *February* 1991)

Abstract—The Sierras Australes (Buenos Aires province, Argentina) form a sigmoidal foldbelt, about 150 km long. The last major orogenic event was Variscan, as shown by synsedimentary folds in upper Palaeozoic sediments and by K–Ar or Rb–Sr ages on cleavage-forming minerals of low metamorphic grade. Folds in the Paleozoic cover are associated with cleavage, stretching lineation and kinematic indicators (shear bands and sigmoidal tails around porphyroclasts). Reworking of the granitic Precambrian basement resulted in shear zones and faults.

We distinguish three structural domains within the Sierras Australes: a Northwestern Arc, a Southeastern Basin and a Central Belt. The Northwestern Arc is a simple fold-and-thrust belt, verging towards the NE. The Southeastern Basin is a foreland basin, where an underthrust towards the SW is overshadowed by a right-lateral wrench along strike. Finally, the Central Belt has resulted from a combination of right-lateral wrenching and overthrusting, both in a northerly direction. All three domains may have resulted from a uniform state of transpressive stress.

Although the deformation is strongly partitioned at outcrop, it may be simpler at depth. This is suggested by experiments in which sandpacks are subjected to transpression, by reactivating a single basement fault in oblique (right-lateral reverse) slip. We describe one such experiment where fault blocks rotate counterclockwise about vertical axes, producing arcuate thrusts at the surface. By analogy, we suggest that the Sierras Australes formed in a transpressive context, as a result of oblique-slip reactivation of a deep fault zone Strong partitioning in the upper crust was facilitated by upward splaying of faults.

INTRODUCTION

STRUCTURAL studies throughout regions of deformed rocks have often shown that the deformation and its history, the motion, are partitioned. Instead of being homogeneous in space or simply repeating, they are separated into components, each component being dominant in a specific subregion. Hence a study of one subregion alone will not yield information that is valid at regional scale. The dimensions of the region considered are in principle quite arbitrary: partitioning can occur at the scale of crystals, or of continents.

In this paper, we consider partitioning of motions at a regional scale of tens of kilometres, in a tectonic context of transpression. Transpressive motion has components of wrenching and of crustal thickening (Sanderson & Marchini 1984). For particular combinations of ductile wrenching and thickening, total strains have been analysed in detail (e.g. Brun & Burg 1982, Sanderson 1982). To what extent can the components become partitioned at a regional scale? The question has already been addressed in a purely brittle context, where parallel thrust faults and strike-slip faults are active simultaneously, as in positive flower structures. These have been reproduced in experiments with scale models (Emmons 1969, Naylor *et al.* 1986, Richard & Cobbold 1989). Less emphasis has been placed on partitioning at deeper crustal levels, where rocks are ductile. Studies of such partitioning can be done in old transpressive belts, now exhumed by erosion. A major advantage of ductile rocks over brittle rocks is that shear criteria are more readily available and more reliable, especially at low metamorphic grades.

In this paper, we describe partitioning of transpressive motions in a Variscan foldbelt, the Sierras Australes of central Argentina (Fig. 1). This foldbelt is particularly well exposed (Fig. 2). It was eroded in the Early Mesozoic; then was preserved, by burial under later sediments. The present landscape is therefore mostly an exhumed Triassic one, with desert weathering surfaces and ventifacts. The exposed foldbelt has a strikingly sigmoidal shape. We distinguish three areas with differing tectonic styles: the Northwestern Arc, the Central Belt and the Southeastern Basin (Fig. 2). The rocks at outcrop are of low to very low metamorphic grades and this metamorphism is Variscan. Shear zones and shear criteria are abundant, both in the reactivated Precambrian basement and in its Palaeozoic sedimentary cover. Folds are ubiquitous in the cover. These conditions make the foldbelt ideal for studies of partitioning.

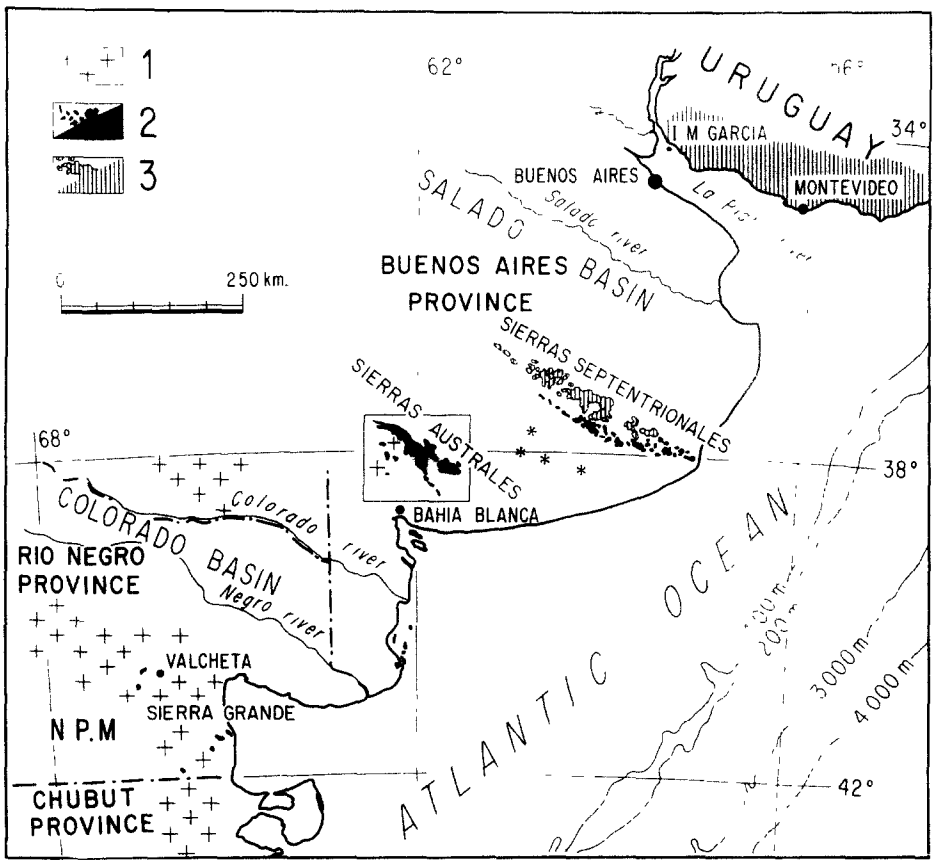

Fig 1 Sketch map of east central Argentina and southern Uruguay, showing main outcrops of Palaeozoic granitoids (1), Palaeozoic sediments (2) and Precambrian basement (3). Sierras Australes foldbelt (central box) is surrounded by Cenozoic sediments (white areas). To the northeast of Sierras Australes, the lowland area as far as Sierras Septentrionales is underlain by a Palaeozoic basin of unknown thickness that outcrops only at a few scattered localities (four stars) To the southwest of Sierras Australes, the nearest exposures of Palaeozoic sediments are near Valcheta and Sierra Grande, on the edge of the North Patagonian Massif (N.P.M.)

GEOLOGICAL SETTING

Because of their geographical location, accessibility and excellent conditions of outcrop, the Sierras Australes have been well studied geologically. Mapping at 1 : 200,000 was done by Harrington (1947) and Furque (1973). There are two regional reviews in Spanish (Llambías & Prozzi 1975, Harrington 1980) and a regional map compiled by Suero (1972). Five recent articles in English deal with tectonic and metamorphic aspects (Cobbold *et al.* 1986, Buggisch 1987, Sellés Martínez 1989, Von Gosen & Buggisch 1989, Von Gosen *et al.* 1991).

Igneous basement

Igneous rocks outcrop in the innermost part of the Northwestern Arc, as a series of small isolated exposures (Fig. 2) Five of these are dominantly of granitic rocks. Three granites (Agua Blanca, Cerro Pan de Azúcar and Cerro San Mario) have yielded Late Proterozoic ages (ranging from 574 ± 10 to 671 ± 35 Ma), by Rb–Sr on whole rock, K–Ar on whole rock, or K–Ar on muscovite (Cingolani & Deutsch 1973; see review by Cobbold *et al.* 1986). Another granite (Cerro Colorado) has yielded an Early Devonian to Late Silurian age (392–417 Ma by Rb–Sr on whole rock). Finally one granite (López Lecube) has yielded Triassic ages (227 ± 32 Ma by Rb–Sr on whole rock and 245 ± 12 Ma by K–Ar on hornblende). The two northwesternmost exposures (La Mascota and La Ermita) are of volcanic rocks. They have yielded Early Carboniferous ages (317–348 Ma), by Rb–Sr on whole rock; Permo-Triassic ages (221 ± 6 and 249 ± 8 Ma) by K–Ar on whole rock (Varela & Cingolani 1975).

Palaeozoic sedimentary cover

The Palaeozoic cover is a succession of dominantly clastic sedimentary rocks, divided by Harrington (1947) into three major groups: from top to bottom, the Pillahuincó, Ventana and Curamalal Groups (Fig. 2). On good fossil evidence, the upper part of the Ventana group (Lolén Formation) is Early Devonian (Emsian) and marine; whereas the Pillahuincó group, which begins with glaciomarine mixtites of the Sauce Grande Formation, is Carboniferous to Permian (possibly even Early Triassic). Recently, Buggisch (1987) has described extremely large trace fossils in the Curamalal group and has attributed them to the Lower Palaeozoic (probably Ordovician). Throughout the Sierras Australes, the Palaeozoic sequence now has a regional sheet dip towards the NE. The palaeoslope was initially towards the SW (Reinoso 1968), but became tilted into a north-

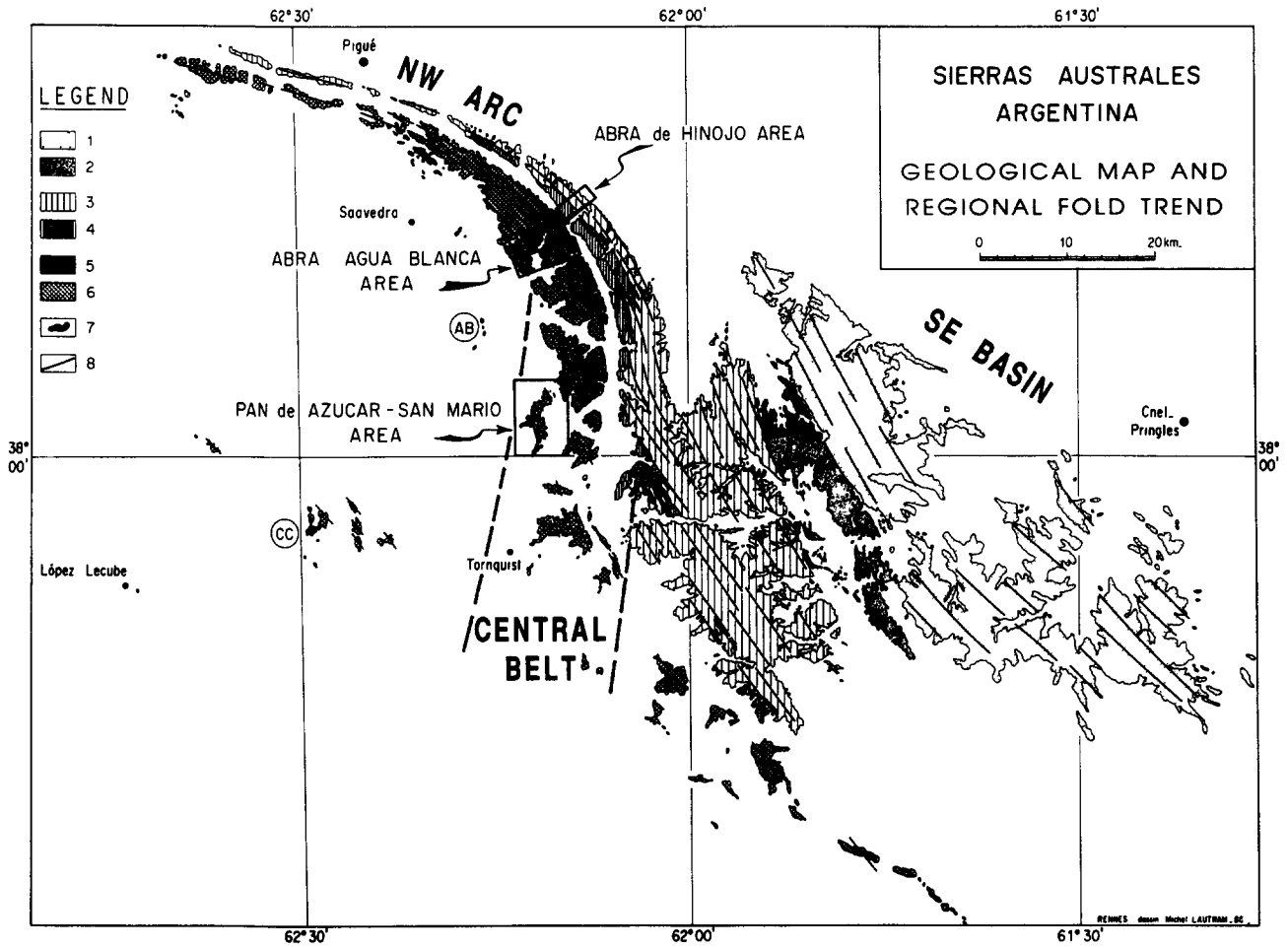

Fig. 2. Sierras Australes. Outcrop map (after Suero 1972) shows main geological formations, tectonic areas and regional fold trends. Within uppermost Pillahuincó Group are Permian sediments of Tunas, Bonete and Piedra Azul Formations (1) and Carboniferous Sauce Grande Formation (2). Within intermediate Ventana Group are Devonian Lolén Formation (3) and Providencia, Napostá and Bravard Formations (4). Within lowermost Curamalal Group are Hinojo Formation (5) and Trocadero, Mascota and La Lola Formations (6). These overlie igneous basement, dominantly Precambrian (7). Axial traces of folds are shown as thick lines (8). Three tectonic areas (Northwestern Arc, Central Belt and Southeastern Basin) are described in text. Boundaries between them (dashed lines) are approximate only. Three subareas (boxes) have been mapped in detail. Quarries in granitic basement at Agua Blanca (AB), Cerro Colorado (CC) and San Mario (large box) were used for studies of shear zones.

easterly dip during the Carboniferous (Coates 1969). The uppermost Pillahuincó group is now preserved in a northeastern synclinal basin (Fig. 2).

Metamorphism

Both basement and cover rocks have undergone regional metamorphism. In general, the metamorphic grade increases with stratigraphic depth, from diagenesis in the Pillahuincó Group, through very low grades in the Ventana group, to lower greenschist grade (with new illite and chlorite) in the Curamalal group and the basement (Fig. 3, after Lluch 1976; see also the recent but comparable results of Von Gosen *et al.* 1991). The higher grades are accompanied by strain and by dynamic recrystallization of detrital quartz grains (Buggisch 1987, Von Gosen *et al.* 1991). Maximum grades occur in the Central Belt and on the concave side of the Northwestern Arc (compare Figs. 2 and 3).

Cobbold *et al.* (1986) and Buggisch (1987) have independently concluded that the main metamorphism and

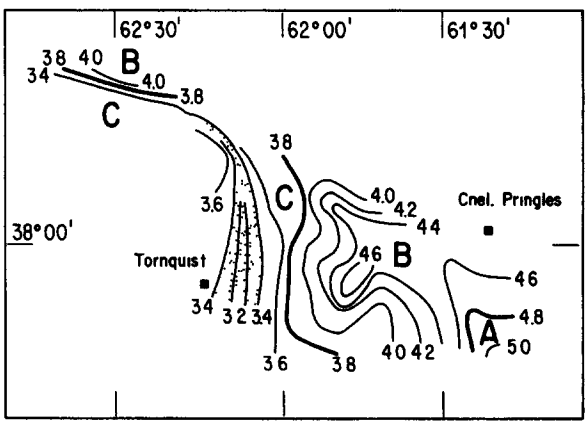

Fig. 3. Low-grade metamorphism in Sierras Australes (after Lluch, 1976). Contours of illite crystallinity index have been used to separate areas of diagenesis (A), very low-grade metamorphism (B) and lower greenschist facies (C). Notice Central Belt, trending N–S (stippled), where crystallinity index reaches smallest values (less than 3.4).

ductile deformation in Sierras Australes is of Permo-Triassic age. Two fine fractions of illite from the Mascota quartzites (Curamalal Group) have yielded K–Ar ages of 260 ± 3 and 282 ± 3 Ma (Buggisch 1987). Others have yielded 273 ± 8 and 265 ± 8 Ma (Varela *et al.* 1985).

Tectonic styles and interpretations

Throughout the Palaeozoic cover, the most striking structures at outcrop are folds (Figs. 4a & c); so much so, that Harrington (1947) considered the Sierras Australes to be the purest example of a foldbelt, with few or no faults. Cleavage and stretching lineation are very common, especially where rocks reach greenschist grade. True slaty cleavage occurs in the Sauce Grande mixtites and Hinojo slates (Fig. 4b). Cobbold *et al.* (1986) mapped the cleavage and lineation at regional scale (Fig. 6). They described ductile shear indicators (Figs. 4d and 5) and used them to identify thrust zones, top to the NE, and right-lateral wrench zones, trending N–S. On this basis, they interpreted the Sierras Australes as a right-lateral transpressive foldbelt of Variscan age. Sellés Martínez (1989) also favoured a transpressive origin, but by left-lateral wrenching in an E–W direction. He showed little field evidence for this, relying mostly on plate tectonic arguments and on geometric similarities with analogue models. Von Gosen & Buggisch (1989) recognized both thrusts and wrench zones, but concluded that the wrench zones formed later than the thrusting.

THE NORTHWESTERN ARC

The Northwestern Arc is a remarkably regular structure (Fig. 2). The somewhat asymmetric outcrop pattern is controlled by the geometry of folds in the cover rocks. Fold axes are gently plunging, forming a regional pericline (Harrington 1947). Hence most formations show maximum outcrop widths in the central part of the arc. Indeed, the uppermost formation of the Curamalal Group (Hinojo slates) is preserved nowhere else. Cleavage strikes nearly parallel to the arc, except towards its southeastern end, where cleavage becomes quite oblique (Fig. 6, top). Similarly, the stretching lineation is mostly perpendicular to the arc, except towards its southeastern end, where the lineation becomes almost along strike (Fig. 6, bottom). Thus the arc is asymmetric in terms of strain, as well as outcrop shape.

In the central part of the arc, we have mapped in detail two traverses: one through the Curamalal Group, the other through the Ventana Group (see location boxes, Fig. 2). For each traverse, we used air photographs and transferred the geological information onto a 1 : 50,000 topographic base (Fig. 7, top and Fig. 8, top). Next we drew three parallel geological sections, along lines perpendicular to the regional fold trend and about 1 km apart. To obtain accurate fold profiles, we used additional photographs, taken at a series of well-located field stations, with views along fold plunges (Fig. 4a). Finally, the three geological sections were projected down plunge onto a single plane (Fig. 7, bottom and Fig 8, bottom)

The resulting sections are more detailed and probably more accurate than the ones previously published for the Sierras Australes by Harrington (1980) or Suero (1973). Our sections show folds of chevron style, with straight limbs, angular hinges and nearly constant bed thicknesses. The folded sediments are mostly well-bedded quartzites, with little internal strain. They have folded by a mechanism of flexural slip. The folds are asymmetric: axial surfaces dip SW, but the enveloping surfaces dip NE. Hence short limbs are steep to overturned. The degree of overturning increases towards the NE (compare Figs. 7 and 8). In the Providencia Formation (Fig. 8), axial surfaces flatten with depth, suggesting décollement. Near the base of the Hinojo Formation (Fig. 7), there are many pelitic horizons. Here the rocks have a pronounced slaty cleavage and a steeply pitching stretching lineation (Fig. 4b). At outcrop and in thin section, there are flat-lying shear bands, indicating thrusting, top to the NE. Hence all the structures in this central part of the Northwestern Arc are typical of a simple fold-and-thrust belt. Nowhere here is there evidence of significant wrench deformation along strike.

Fold amplitudes and strains appear to decrease progressively towards the NW. The final exposures west of Pigüé (Fig. 2) show little deformation. In contrast, from the centre of the arc towards the SE, there is little change in the intensity of deformation, only changes in style and attitude that will be described later. These features show once again that the arc is asymmetric.

THE SOUTHEASTERN BASIN

Regional sections through the Southeastern Basin by Harrington (1947, 1980), Furque (1973) and Suero (1972, 1973) have been reproduced by Cobbold *et al.* (1986), Buggisch (1987) and Sellés Martínez (1989). They will not be illustrated here. From NE to SW, the regional sections show an irregular increase in the intensity of folding.

In the eastern part of the basin, detailed sections through the folded Carboniferous and Permian sediments of the Pillahuincó Group have been published recently by Japas (1986, 1987). Line balancing has yielded a regional horizontal shortening of no more than about 10%. The Sauce Grande Formation (Carboniferous) is here about 1000 m thick; the Permian, at least 1600 m. From SW to NE, the stratigraphic thicknesses of both Carboniferous and Permian sediments appear to increase, suggesting that basin formation was active during the Late Palaeozoic.

At one locality with Permian sediments (railway bridge near Zoilo Peralta, 38°04'S, 61°42'W), we have observed growth folds, with depocentres in synclines and condensed sequences over anticlines. These indicate coeval sedimentation and compressional deformation of Permian age. In general, cleavage in the

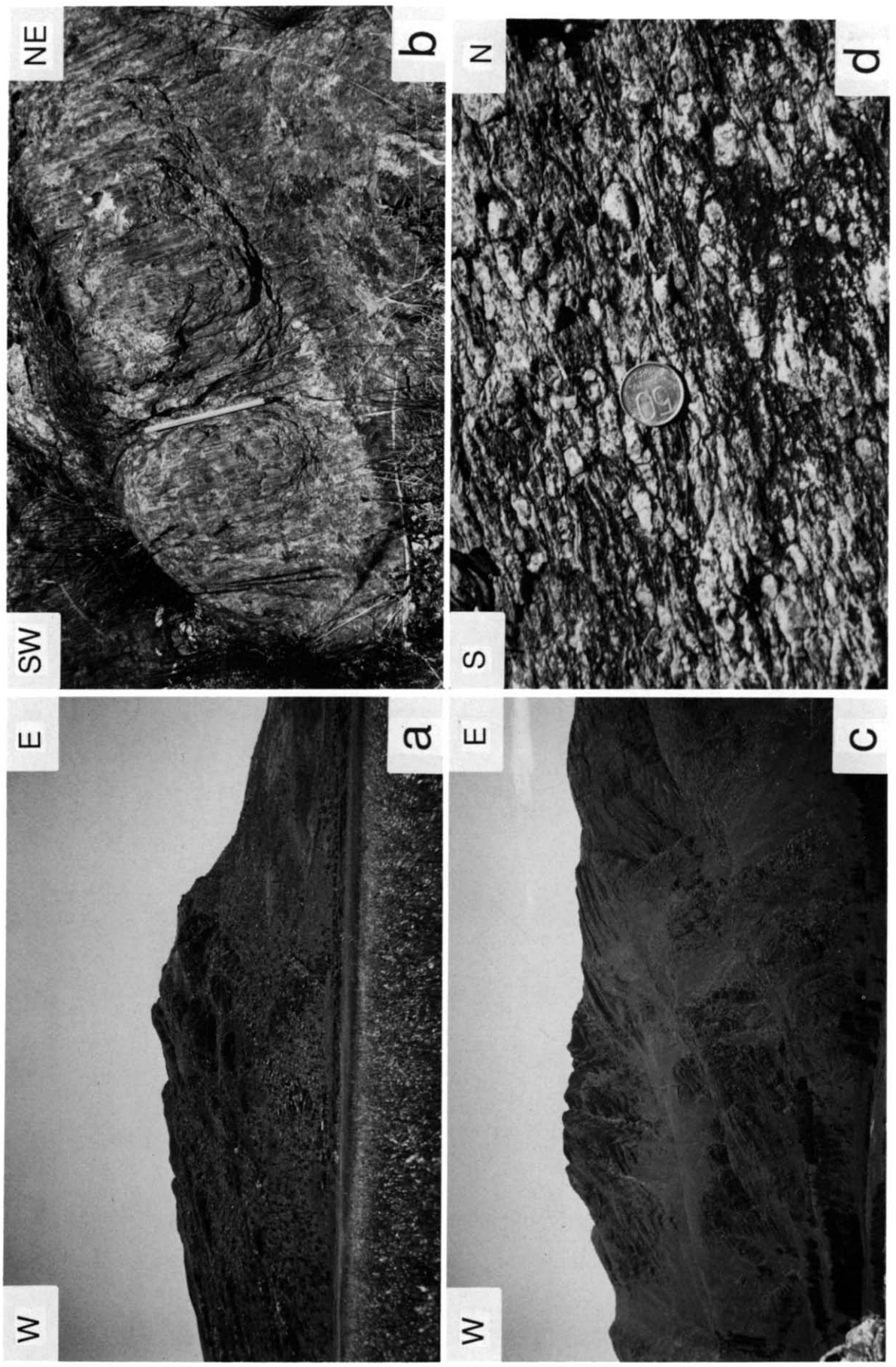

Fig. 4. Structures at outcrop in Northwestern Arc (top) and Southeastern Basin (bottom). (a) Flat-lying folds and overturned (thrusted) contact between Trocadero and Hinojo Formations, roadside locality, Abra La Sofia (southernmost outcrops of Hinojo Formation, 62°06'W, 37°53'S). Vertical relief is about 100 m. (b) Cleavage and stretching lineation in mylonitic Hinojo slates, Abra La Sofia (view towards the east, same locality as a). Cleavage dips about 40°WSW; lineation pitches 75°SE (along pencil). This indicates dominant overthrusting towards the NE, with minor right-lateral wrenching (c) Upright folds in quartzites of Ventana Group, locality south of road in Abra de la Ventana (61°57'W, 38°12'S) Chevron folds are somewhat asymmetric, with axial surfaces dipping SW, short limbs vertical to overturned, long limbs more gently dipping. This indicates minor component of thrusting, top-to-NE. Vertical relief is about 800 m (d) Right-lateral shear bands within mylonitic steep limb of fold in quartzites of Ventana Group (view vertically downwards, locality south of road, Abra de la Ventana, 62°01'W, 38°45'S). This indicates a component of right-lateral wrenching coeval with folding

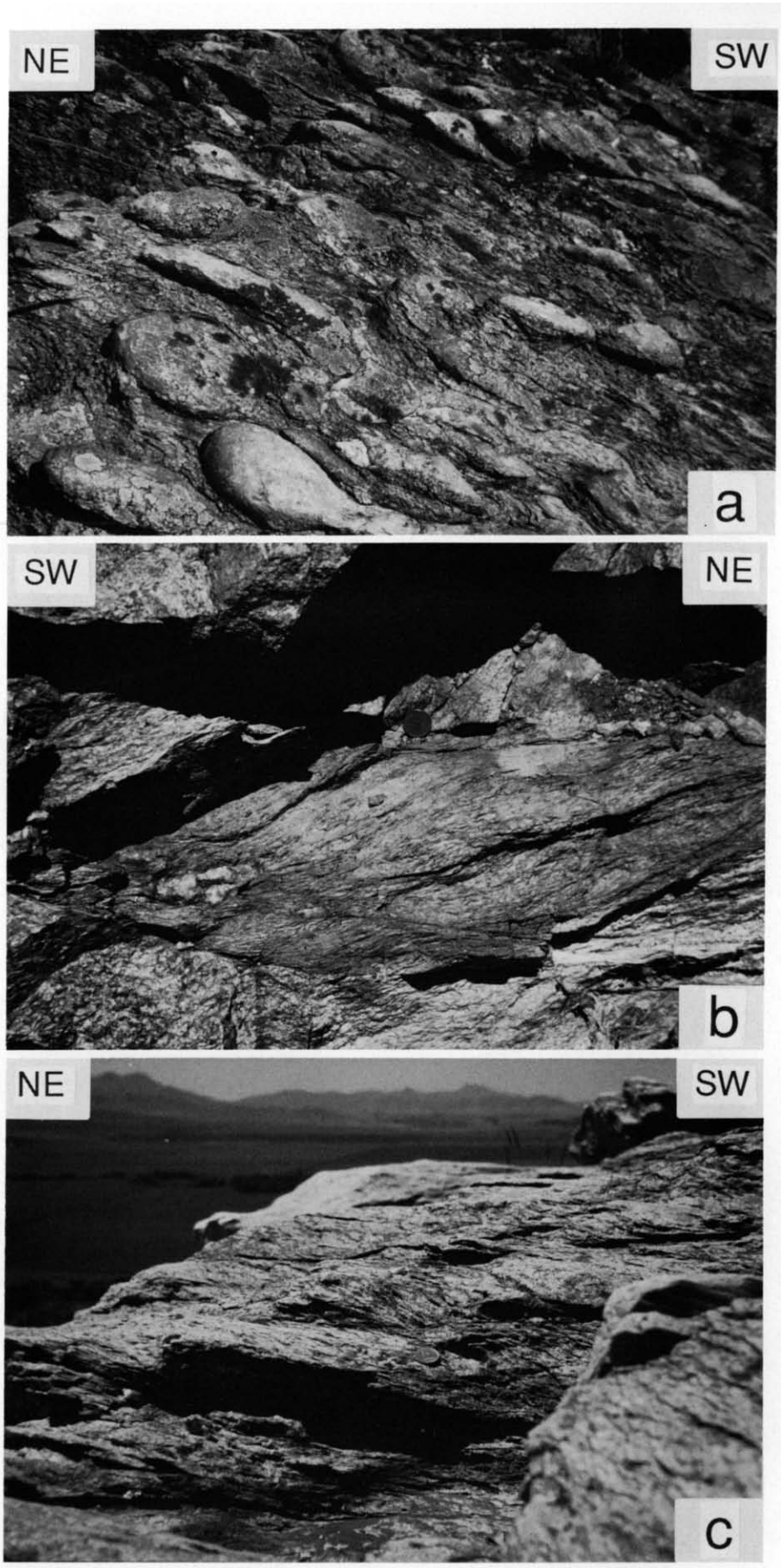

Fig 5 Structures at outcrop in Central Belt (a) Cleavage and single set of shear bands in La Lola conglomerate at Cerro del Hueco (for location, see Fig. 9). Cleavage dips at about 30° towards SW; shear bands are flat-lying. Pebbles are flattened in cleavage; they are also stretched along lineation, which pitches about 60°SE Asymmetric pebbles and shear bands indicate oblique motion (right-lateral, top to NE) (b) Right-lateral steep shear bands and cleavage of greenschist grade in granitic basement at Las Lomitas quarry (for location, see Fig 9) View looking downwards. These structures indicate a component of right-lateral wrenching along strike (c) Flat-lying cleavage and shear bands in quartzites of Mascota Formation, southern end of outcrops near Estancia San Mario (Fig 9) View is almost perpendicular to stretch lineation itself parallel to reorientated axes of tubular folds Shear criteria indicate thrusting, top-to-NNE

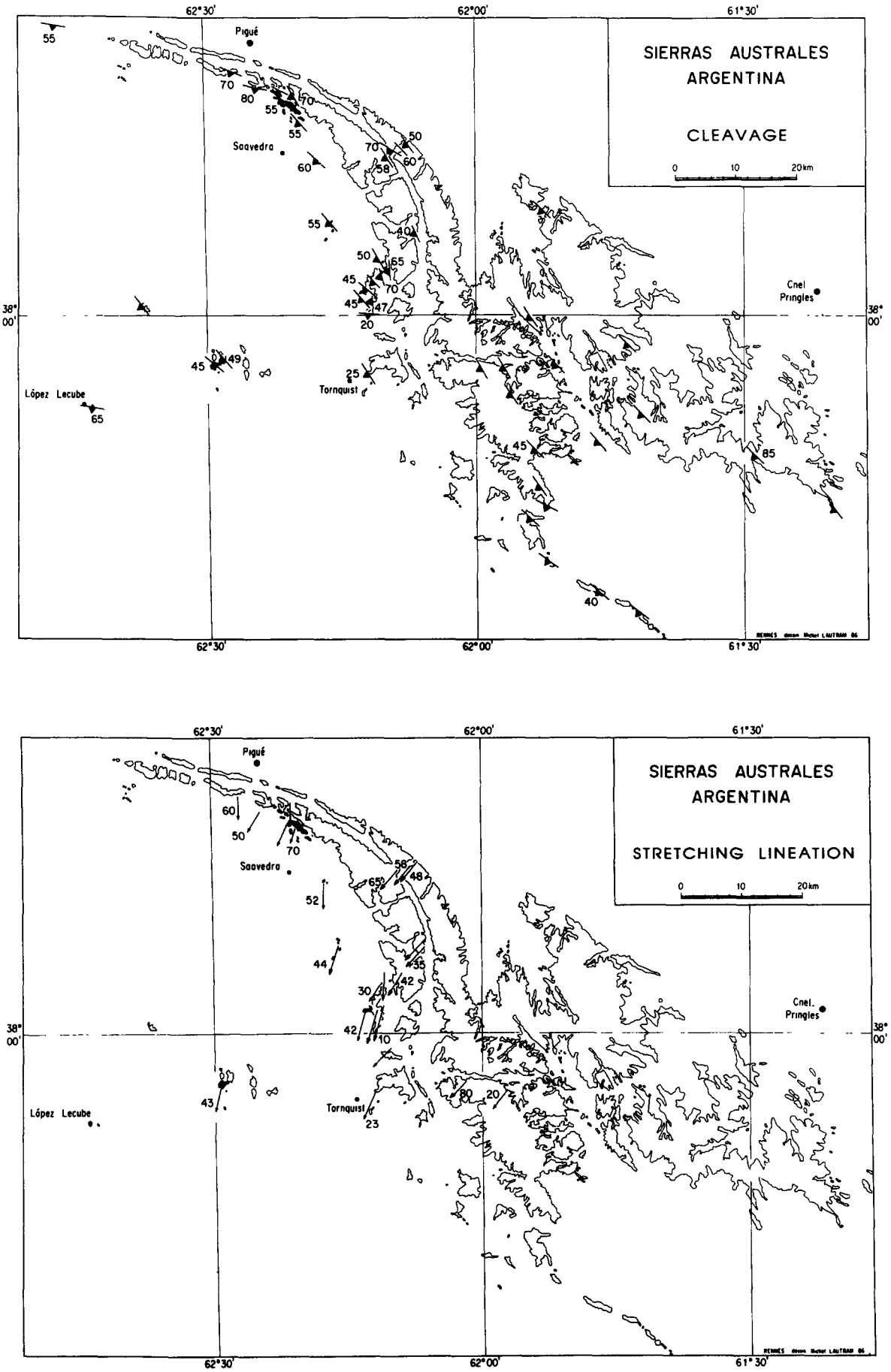

Fig. 6 Maps showing dip of penetrative cleavage (top) and plunge of stretching lineation (bottom). Data from Cobbold *et al.* (1986), with recent unpublished additions.

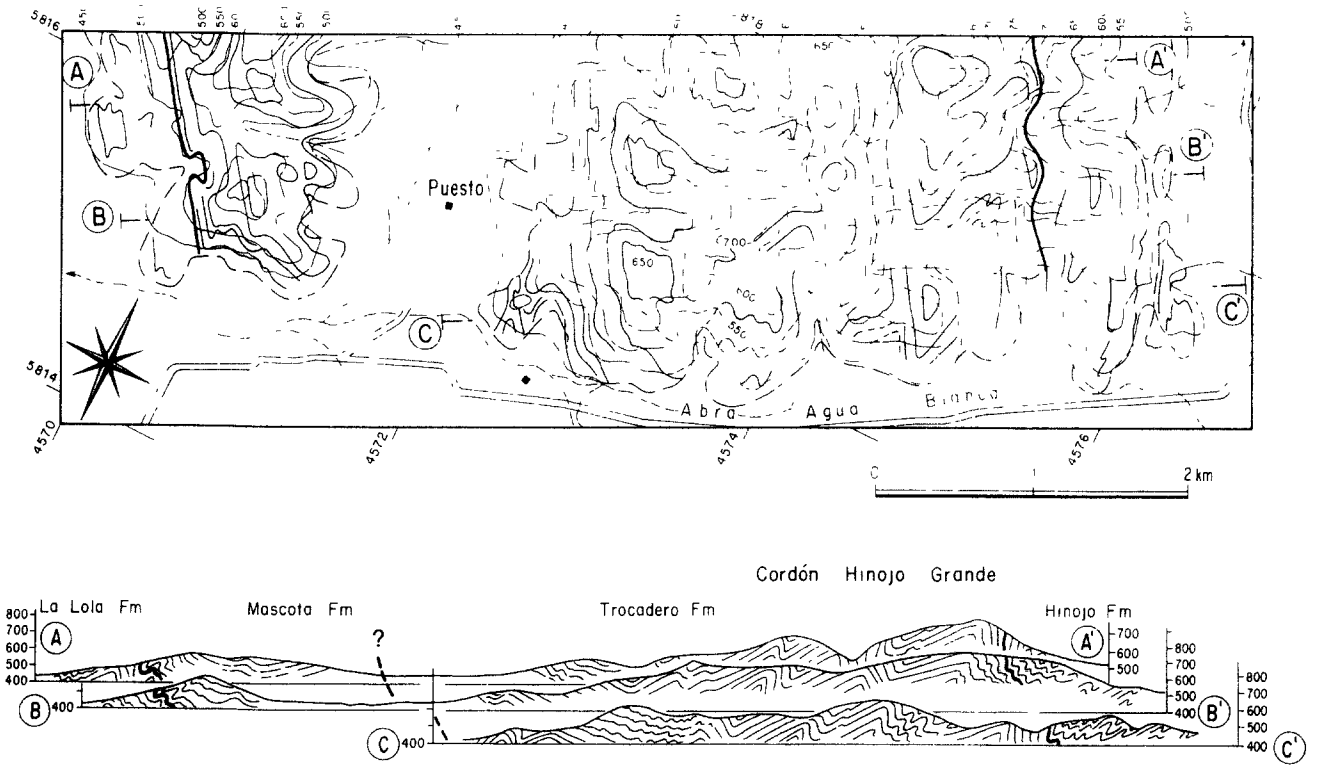

Fig. 7 Traverse through Abra Agua Blanca For location, see box (Fig 2) Map (top) shows topographic contours (thin continuous lines, labelled in metres), roads (parallel lines), streams (arrows pointing downstream) and geographic grid lines, all taken from 1 50,000 topographic maps of the Instituto Geográfico Militar. We have added outcrop boundaries (alternating dots and dashes), bedding traces (thick lines, continuous where observed, dashed where inferred) and geological boundaries (thickest lines). We have drawn three parallel geological sections (A–A', B–B' and C–C') and projected them down the regional plunge of fold axes onto a single section (bottom) This section shows folded bedding (thin lines) and formation boundaries (thick lines) Vertical scale (labelled in metres) is same as horizontal scale. For an example of photograph used in drawing sections, see Fig. 4(a)

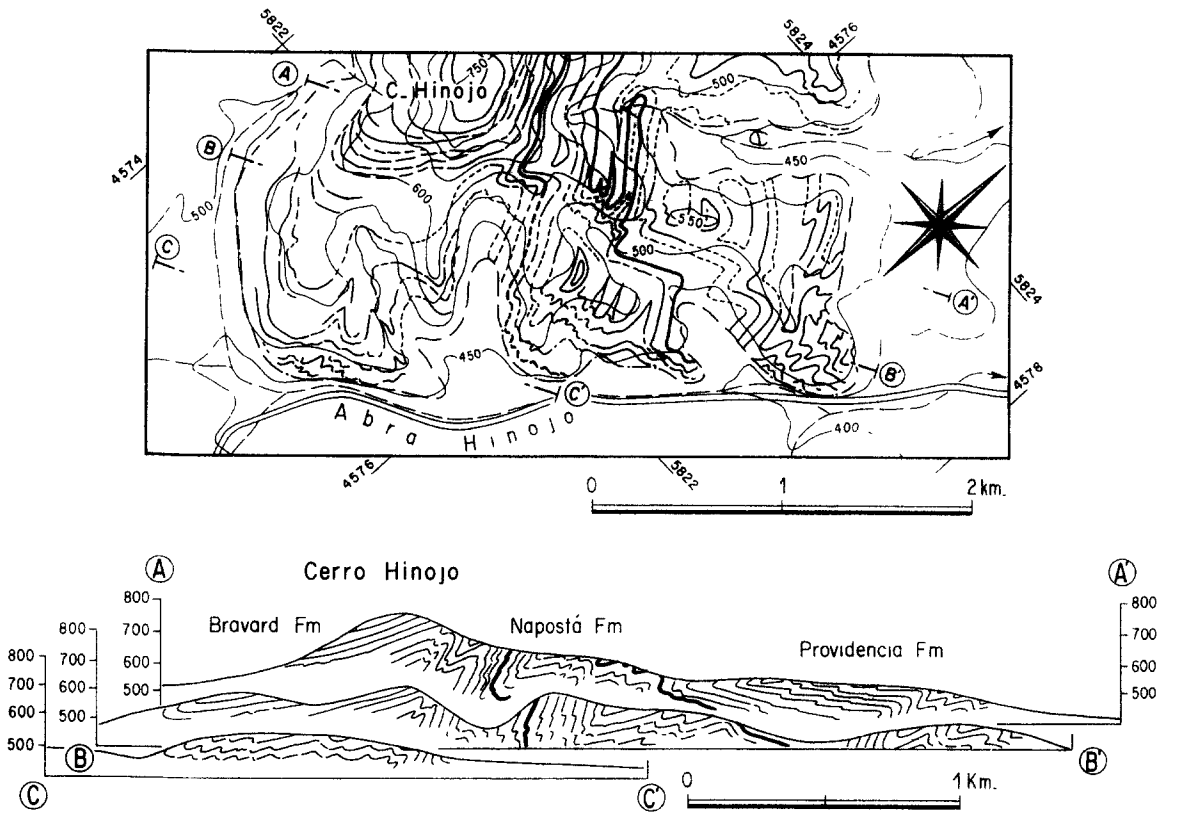

Fig 8 Traverse through Abra de Hinojo. For symbols, see caption to Fig 7

Permian is incipient and widely spaced. The direction of maximum stretch, obtained from deformed fossils, is often horizontal and parallel to fold axes (Japas 1986). At the growth fold locality (Zoilo Peralta), there is anticlockwise transection of fold axes by cleavage. The transection angle is small on fold limbs, but reaches a maximum of about 30° in the hinge areas. If cleavage and folding were indeed coeval, the transection is best attributed to a component of right-lateral wrench deformation (see discussion and references in Van der Pluijm 1990). Further structural evidence for right-lateral wrench deformation has been presented by Japas (1989).

In the Carboniferous Sauce Grande mixtites, pebbles are mostly derived from Lower Palaeozoic quartzites, with some fragments of granitic basement. This suggests that uplift and erosion were already active during the Carboniferous. The pebbles in the Sauce Grande mixtites are flattened and enveloped by a steep slaty cleavage (presumably Permo-Triassic) developed in the pelitic matrix. The stretching lineation is sometimes steep, sometimes nearly horizontal. At various localities (for example, 61°50'W, 38°00'S), we have observed shear bands, indicating either an overthrust to the ENE, or a right-lateral wrench along strike.

In the western part of the basin, within the quartzites of the Curamalal and Ventana groups, folds are much tighter (Fig. 4c). Here the chevron folds are slightly overturned to the NE, but more upright than in the Northwestern Arc (compare with Fig. 4a). In this area, there are abundant steep mylonitic shear zones within fold limbs (Fig. 4d). In the shear zones, there is a fine-grained matrix of dynamically recrystallized quartz. Sigmoidal tails around clastic grains indicate a component of right-lateral shearing along strike. Hence we interpret deformation in this area as dominantly due to right-lateral wrenching, with subsidiary overthrusting to the NE.

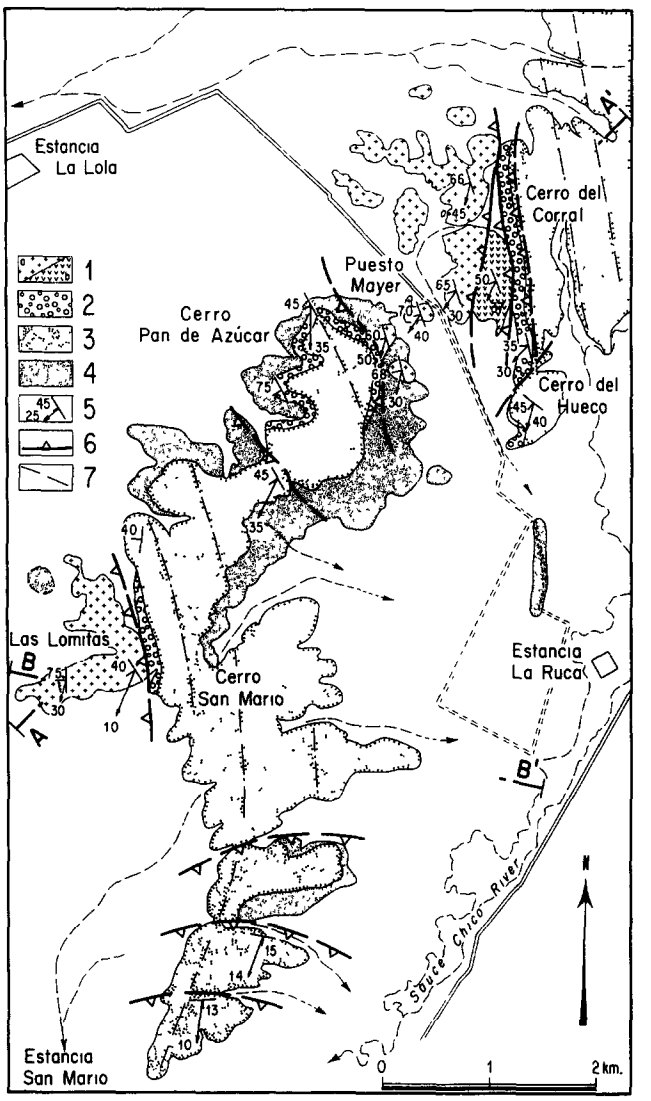

Fig. 9. Geological outcrop map of subarea around Cerro Pan de Azúcar, Cerro San Mario and Cerro del Corral. For location, see large box (Fig. 2) Formations are rhyolitic basement (1a), granitic basement (1b), La Lola conglomerate (2), Mascota quartzites (3) and scree deposits (4). Structural features are dips of penetrative cleavage surfaces and plunges of stretching lineations (5), traces of major mylonitic shear zones and faults (6) and axial traces of major folds (7)

THE CENTRAL BELT

We believe that observations in this belt are important to understanding the formation of the Sierras Australes. The belt runs approximately N–S, from the quartzite outcrops east of Tornquist, to the subarea around Pan de Azúcar and Cerro San Mario (Fig. 2). We have mapped this subarea in detail (Fig. 9), incorporating earlier data of Cucchi (1966) and Varela *et al.* (1986). We have also compiled two geological sections (Fig. 10). One of these runs NE–SW, approximately parallel to the trend of the stretching lineation in this area; the other section is almost perpendicular to it. This subarea is the only one that shows contacts between the Precambrian granitic basement and its Palaeozoic cover. Two high-angle fault zones with reverse components put the basement on top of the cover (Fig. 10). At Cerro Pan de Azúcar, the La Lola conglomerate, 100 m thick and little deformed, rests unconformably on the basement, via a more flat-lying thrust zone containing mylonitized basement and cover rocks (Fig. 10). At Cerro del Corral (Fig. 10) and Cerro del Hueco (Fig. 9), the La Lola conglomerate is overturned to the SW. The pebbles are strongly flattened within a gently dipping cleavage and are elongate parallel to a stretching lineation that pitches southwards (Fig. 5a). Well-developed flat-lying shear bands, offsetting small pebbles, indicate overthrusting to the NE, combined with right-lateral wrenching along strike.

Combinations of thrusting and wrenching can be recognized also in the basement. In quarries at three localities, the basement is cross-cut by shear zones (Fig. 5b). Microstructures are typical of water-assisted mylonitization under metamorphic conditions typical of lower greenschist facies. Quartz grains show core-and-mantle structures due to recrystallization at grain boundaries. Quartz *c*-axes, subgrain boundaries and kink-bands are all at low angles to the principal shortening direction, indicating that ⟨*a*⟩ slip was the dominant

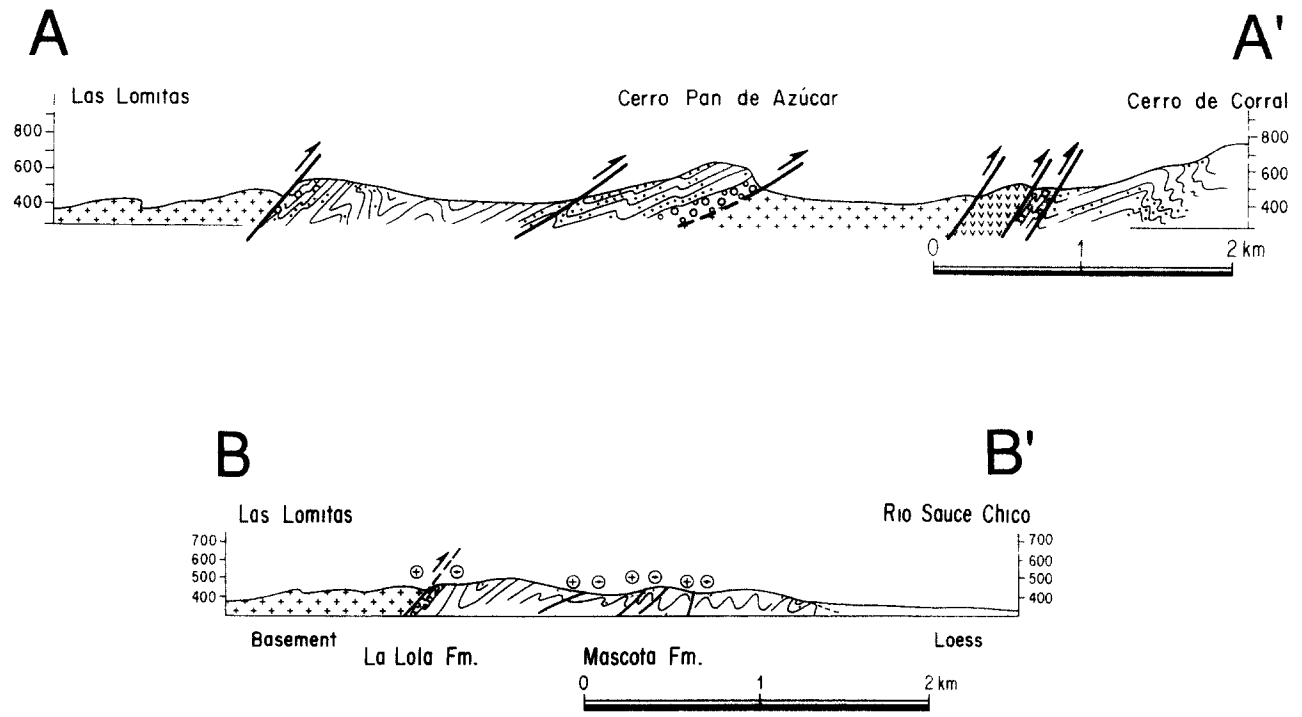

Fig 10. Geological cross-sections through subarea around Cerro Pan de Azúcar, Cerro San Mario and Cerro del Corral. For location of section lines and for geological ornament, see Fig. 9. Line A–A′ is at small angle to trend of stretching lineation; line B–B′, nearly perpendicular to it. Thin folded lines are bedding traces; thicker lines indicate major mylonitic fault zones, either dominantly reverse (half arrows), or dominantly strike-slip (symbols in circles. crosses, for motion away from observer; arrow tips, for motion towards observer) Vertical scale (labelled in metres) is same as horizontal scale.

deformation mechanism. Feldspars show brittle fractures, but also have broken down into fine-grained assemblages rich in white mica. The assemblages appear to have been the weakest component of the mylonites. All these features indicate that temperatures within the Central Belt did not exceed 300–400°C (Mitra 1984, Simpson 1985, Janecke & Evans 1988, Gapais 1989). For the shear zones in the basement, we were able to make detailed measurements of the attitudes of shearing planes and shear directions and to recognize the senses of shear (Fig. 11). The shear zone distribution shows a degree of orthorhombic symmetry, with four main families of shear zones: flat-lying zones, top to the NE (Z1); steep zones, southwestern side down (Z2); moderately steep zones, dipping SW, right-lateral (Z3); and steep zones, dipping SSW, left-lateral (Z4). We used the method of superposed compressional or extensional dihedra (Pfiffner & Burkhard 1987) to find principal directions of shortening or of extension. In so doing, we made no assumptions concerning the state of stress. We believe the method is more likely to estimate the state of strain, provided the strain magnitudes are small. This condition appears to be met in the granitic basement, where the density of shear zones and the amounts of displacement upon them do not seem large. The results of our analysis are compatible with the attitudes of cleavage and stretching lineation in the basement rocks (Fig. 11). We infer a principal shortening that plunges about 30° northeastwards; and a principal extension that plunges about 45° southwards. Notice that in all three stereograms, the contours for the extension field define a great circle girdle. From this we infer a strain ellipsoid of oblate shape. Shear zone families Z1 and Z2 are conjugate and intersect nearly along the intermediate strain axis. Families Z3 and Z4 are conjugate and intersect nearly along the major strain axis. However, all orientations are not equally populated. Instead, families Z1 (low angle thrusts) and Z3 (right-lateral wrenches) are each more numerous than their conjugates. Hence the overall symmetry is not really orthorhombic, but triclinic. Also there are many shear zones of intermediate orientations, where overthrusts to the NE and right-lateral wrenches are combined. This becomes clear when we plot the pitch of the shear direction against the strike of the shearing plane (Fig. 12). The plot uses a pitch of 45° to separate fields where either thrusting or wrenching has predominated. We have grouped the two dominant families (Z1 and Z3), to illustrate the transition between them.

In the southernmost part of the subarea (from Las Lomitas to Estancia San Mario, Fig. 9), quartzites of the Mascota Formation have undergone intense strain (Fig. 5c). Cleavage dips range in direction from south to west (Fig. 13). Where cleavage dips south, it tends to be associated with a steeply pitching stretching lineation; where cleavage dips west, with a gently pitching lineation. For the first association, shear bands indicate overthrusting, top to the N; for the second, right-lateral wrenching. The thrusting is concentrated into three main zones (Fig. 9). It has produced flat-lying folds, superimposed upon earlier upright folds (Fig. 10, section B–B′). The early fold axes trend north and have associated right-lateral shear indicators. In these quartzites, therefore, we have evidence for superposition of

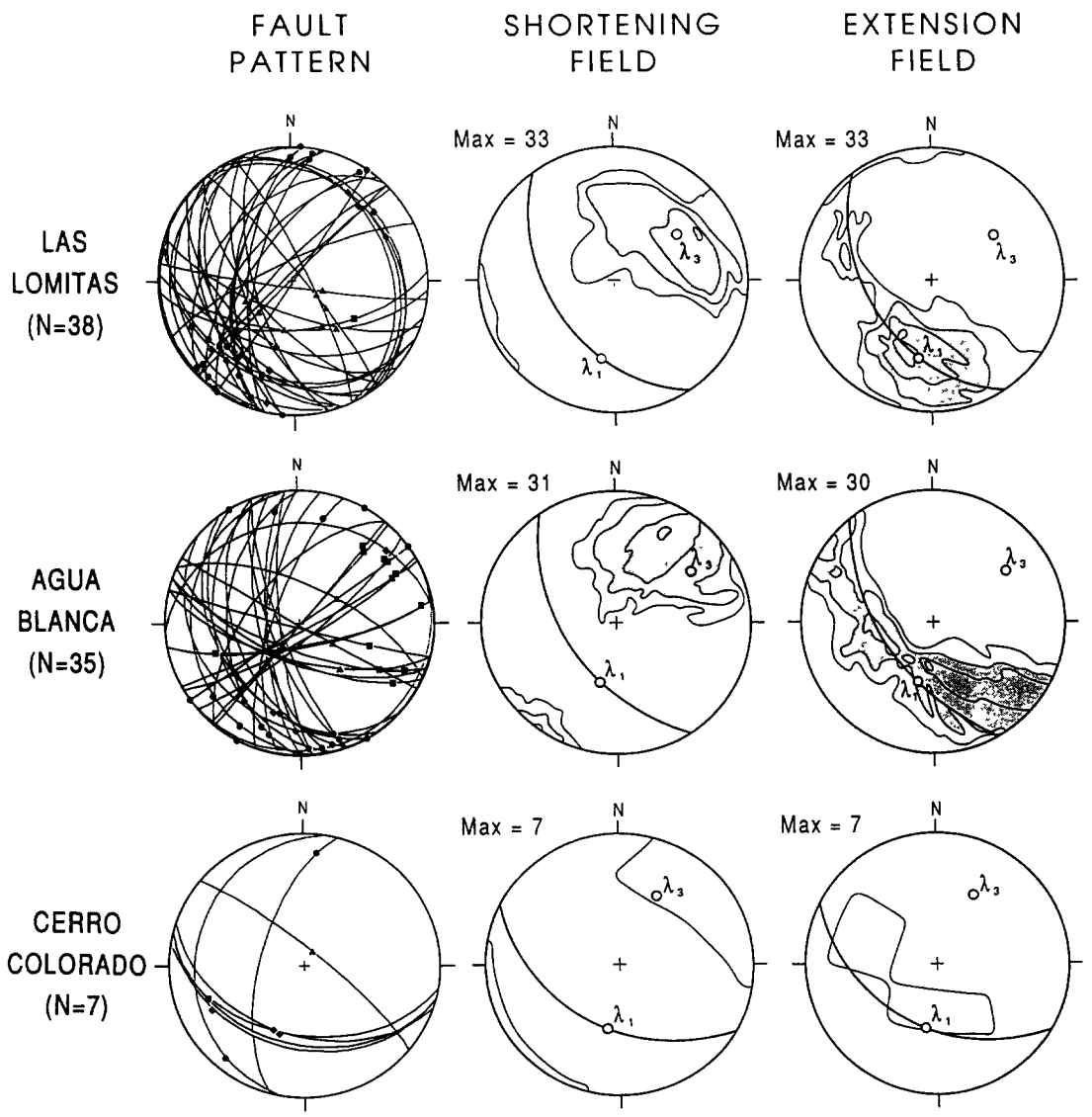

Fig. 11 Attitude and kinematic significance of mylonitic shear zones in basement rocks (stereographic projections, lower hemisphere). Localities are Las Lomitas (Fig. 9), Agua Blanca (AB, Fig. 2) and Cerro Colorado (CC, Fig. 2). Number of shear zones measured is labelled *N*. Left-hand column shows orientations of shearing planes (great circles) and of shear directions (full black symbols). There are four main families of shear zones. Family Z1 is flat-lying and sense of shear is top to the NE (diamonds); family Z2 is steep and sense is SW-side-down (triangles); family Z3 dips moderately steeply to SW and sense of shear is right-lateral (circles); family Z4 is steep and sense is left-lateral (squares). Fields of shortening (central column) and extension (right-hand column) have been calculated for shear zone population by method of superposed dihedra (Pfiffner & Burkhard 1987) First, dihedral angle containing shortening (or extension) direction is calculated for each shear zone. Then dihedra for entire population are superposed Contours are for number of superpositions, expressed as percentage of maximum number of superpositions (Max). Contour interval is 10%; first contour is 70%; grey area is above 80%. Great circle represents average cleavage attitude for each locality. Pole to cleavage is inferred to be principal direction of shortening (λ_3); stretch lineation is inferred to be principal direction of extension (λ_1)

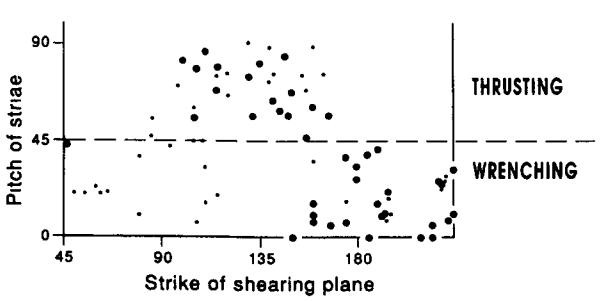

Fig. 12. Pitch of striae vs strike of shearing plane for all shear zones in granitic basement. Pitch of 45° separates fields where either thrusting or wrenching dominates. Shear zones are in two groups: right-lateral or top-to-the-NE (large black dots); and all others (small black dots).

thrusting upon wrenching. Possibly the same superposition has occurred in the basement, but we have no direct evidence for it.

REGIONAL PARTITIONING

The Northwestern Arc, Southeastern Basin and Central Belt show differing states of finite deformation and we have inferred for them differing motions (Fig. 14). The Northwestern Arc has undergone mainly thrusting across strike; the Southeastern Basin, mainly right-lateral wrenching along strike; and the Central Belt, combinations of thrusting and wrenching in a northerly

direction. Geochronological and stratigraphic data nevertheless suggest that the main motions are regionally synchronous and of Permo-Triassic age We therefore infer a partitioning of motion at regional scale The partitioning can be further illustrated by plotting the pitch of stretching lineation against the strike of cleavage for the entire region (Fig. 15) The plot is similar to the one for the San Mario subarea (Fig. 13). Overthrusting at a regional scale has occurred in directions varying between N and ENE; right-lateral wrenching, along directions varying between ENE and S (Fig. 15). This suggests that the degree of partitioning has been considerable, at the upper crustal levels now exposed. It also raises two important questions. First, could the deformation and the motion have been more uniform, at depth? Second, could the state of stress have been more uniform throughout? We believe that experiments with scale models can help answer such questions.

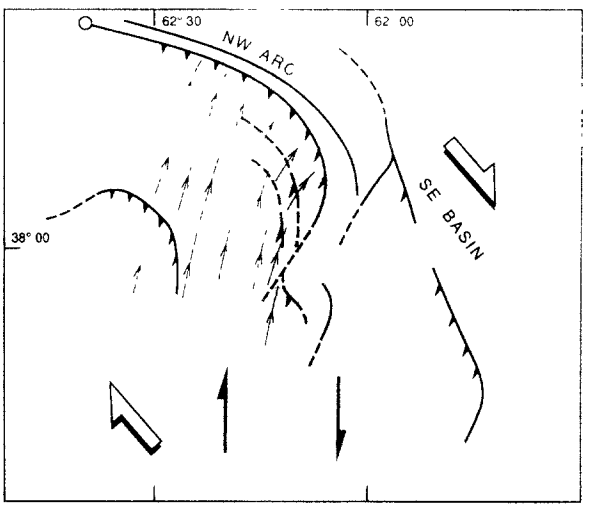

Fig 14 Tectonic sketch map of Sierras Australes We interpret the Northwestern Arc as an asymmetric fold and thrust belt Black triangles on main thrust zone point in directions of underthrusting, which become more and more oblique towards the SE Amount of underthrusting decreases towards the NW until thrust zone terminates (open circle) at pole of relative counterclockwise block rotation Thin trajectories with open arrows are tangent to trend of stretching lineation and may be close to shear directions of minor thrusts. We attribute Central Belt (stippled) to combinations of right-lateral wrenching (pair of black arrows) and overthrusting, both in northerly directions The Southeastern Basin we attribute mainly to right-lateral wrenching along strike On the scale of entire Sierras Australes, we infer that right-lateral wrenching along strike (pair of large hollow arrows) dominated over thrusting

Partitioning in a scale model

The geometry of brittle flower structures in nature and their reproduction in laboratory experiments show that it is indeed possible for fault motions to be simple at depth, but more complex and partitioned at upper crustal levels (Emmons 1969, Naylor *et al.* 1986, Richard & Cobbold 1989). To illustrate this, we will analyse the fault geometry and the displacement pattern in a single experiment, done at the Shell Research Laboratories in The Hague, The Netherlands. New faults were created in a uniform sandpack, above a rigid basement containing a single inclined pre-existing fault. The basement fault was reactivated in oblique (right-lateral reverse) slip (Fig. 16, after Richard 1990, pp. 132–133).

The sand used (quartz sand, from Fontainebleau, France, of grain size about 0.4 mm) is a Coulomb material: its failure envelope in Mohr space is almost perfectly linear, over the range of stresses considered, with an angle of internal friction of about 30° and a cohesion of about 100 Pa (Krantz 1991). Horsfield (1977) has shown that dry sand can be a good analogue for brittle behaviour of rocks in the upper crust: if cohesion and linear dimension scale down by the same factor (here about 2×10^5), body forces and surface forces will be in their correct proportions.

In its undeformed state, the sandpack was 75 cm long, 55 cm wide and 8 cm thick Horizontal marker layers were inbuilt to register vertical motions (Fig. 16a). A square grid of thin sand ridges, 3 cm apart, was laid down on the free surface to monitor surface deformation (Fig. 16b). The sandpack was built up and then deformed on a rigid deformation table, 2 m long and 1.5 m wide. This table is constructed in two halves. One half can be moved past the other, both laterally and vertically in any

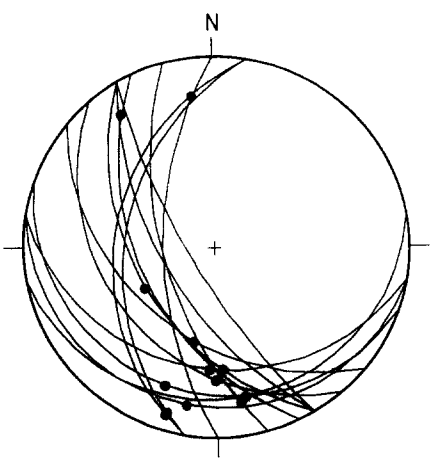

Fig 13 Attitude of cleavage and stretching lineation for San Mario subarea (Fig. 9). Great circles on equal-area stereographic projection represent cleavage; black dots, stretching lineation

Fig 15 Graph showing pitch of stretching lineation vs strike of cleavage for Sierras Australes. Regional data taken from Fig. 6. Pitch of 45° separates fields where either wrenching or thrusting dominates.

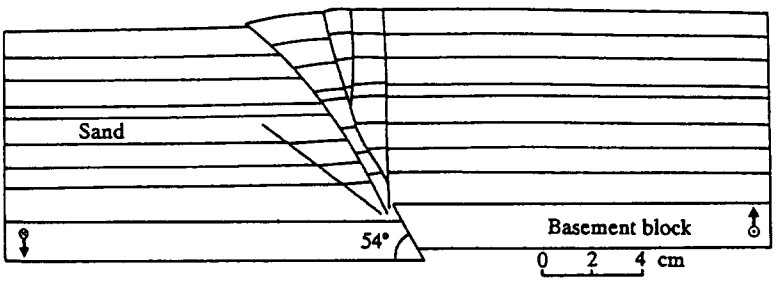

(a)

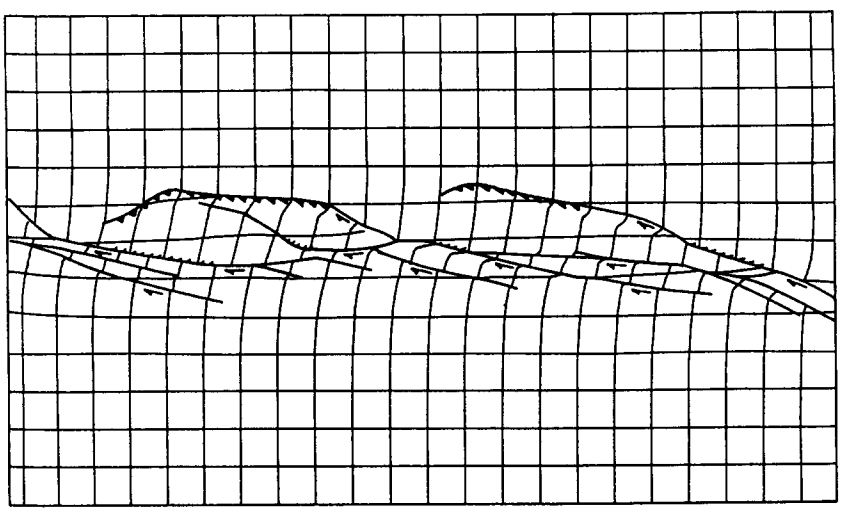

(b)

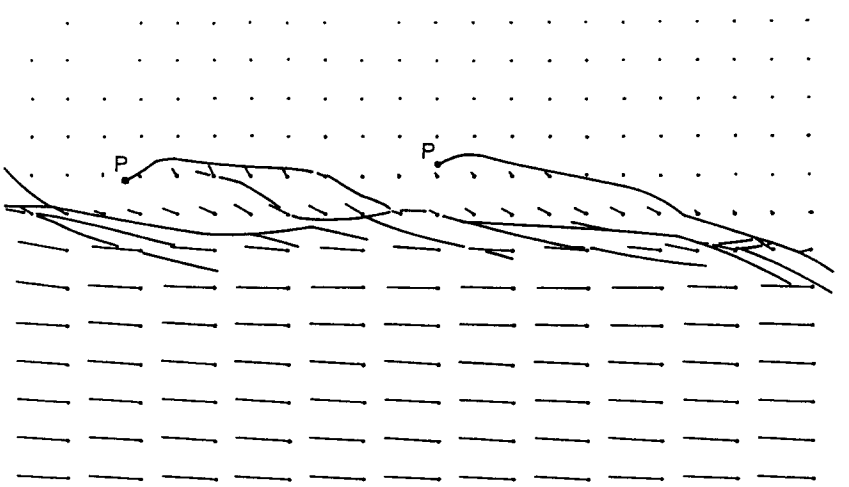

(c)

Fig. 16. Faulting in a sandpack above an oblique-slip (left-lateral reverse) basement fault (line drawings, after photographs by Richard 1990, pp. 132–133). Dip of basement fault is 54°. Total slip on the basement fault has the following Cartesian components: 59 mm of right-lateral strike-slip, 4 mm of horizontal convergence and 6 mm of true vertical displacement. Section (a) through sandpack, perpendicular to basement fault, shows flat-lying sand layers, offset across faults. Faults in sand form network (flower structure) branching upwards from basement fault. Steepest faults show small vertical offsets; they are dominantly strike-slip. Main reverse fault (top left) has a smaller dip (about 45° at surface) and is responsible for the break in slope. Surface view (b) shows grid of surface markers (thin lines), originally square in undeformed state, now deformed and offset across faults (thick lines). Faults are classified as strike-slip (plain lines, with half-arrows to show sense), normal (ticks on downthrown side in direction of throw), or reverse (triangles pointing downdip in direction of throw). Scale is given by spacing of grid lines (3 cm), where grid is still square. Surface view (c) shows vectors of total horizontal displacement (arrows) for selected nodes of surface grid. Vectors are to scale: they span distances between original positions of nodes (dots at bases of arrows) and final positions (points of arrows). Faults (thick lines) separate blocks with nearly rigid behaviour (mainly translations; some rotations). Arcuate reverse faults terminate at poles of relative block rotation (P). Scale is same as in (b).

proportion, so modelling oblique-slip motion on a single basement fault. The dip of the basement fault can be set by varying the attitude of two flaps. For the experiment here shown, the dip was 54° (Fig. 16a). The sides of the sandpack were free, so that the sand there attained a stable surface slope of about 30°.

During the experiment, the basement fault was given a total oblique slip of 60 mm, at a rate of 180 mm h^{-1}. At such small rates, the yield envelope of dry sand is independent of rate. The slip vector had a steady orientation and the total slip had the following Cartesian components: 59 mm of strike-slip, 4 mm of horizontal convergence and 6 mm of true vertical displacement. Thus wrenching overshadowed thrusting. Surface deformation of the sandpack was monitored by time-lapse photography. At the end of the experiment, the sandpack was wetted, to increase the cohesion, then serially cut into vertical slabs (e.g. Fig. 16a)

Viewed at the end of the experiment, the surface showed a zone of deformation, about 10 cm wide, above the basement fault (Fig. 16b). Most of the deformation occurred by faulting. All kinds of faults appeared (normal, reverse, strike-slip and oblique-slip). First to appear at the surface were pure strike-slip faults, at about 20° to the trace of the basement fault. This orientation is predicted by Coulomb theory, assuming a transpressive state of stress, where the intermediate stress is vertically oriented and the principal compressive stress strikes at about 50° to the trace of the basement fault. The strike-slip faults were distributed en échelon, without overstepping. With further deformation, new strike-slip faults formed, more nearly parallel to the basement fault (see Naylor *et al.* 1986). The final fault pattern resembled a strike-slip duplex (Woodcock & Fischer 1986). A feature of interest was that, as deformation accumulated, the original strike-slip faults and intervening blocks rotated about 5° counterclockwise, in domino fashion Counterclockwise rotations of this kind have been described for sandpacks subjected to horizontal plane strain, with combinations of pure shear and right-lateral simple shear (Gapais *et al.* 1991). In those experiments, the faults rotated away from the inferred direction of principal compression In the experiment described here (Fig. 16), strain was not plane; but the rotations were also away from the inferred compression direction. Between the fault blocks and the undeformed material outside the zone of deformation, the relative rotations were accommodated by secondary faulting. Each secondary fault is arcuate. It branches out of a strike-slip fault, sweeps through an angle of up to 60°, then terminates abruptly. The fault is dominantly of reverse type. A map of displacement vectors (Fig. 16c) shows that fault throw increases away from the termination and that slip vectors are somewhat radial with respect to the arc. The pole of relative rotation is thus near the termination of the arcuate fault (P, Fig. 16c). We conclude that domino rotations of blocks about vertical axes are an important aspect of the deformation pattern.

A section through the deformation zone at the end of the experiment shows that all the faults visible at the surface branch up from the basement fault (Fig. 16a) The structure in section is therefore an asymmetric positive flower. Strike-slip faults are nearly vertical; whereas the secondary reverse fault dips at about 45° near the free surface, then curves down into the basement fault The branching upwards of the faults is one reason why the motions become more partitioned towards the surface. Another reason of course is that primary strike-slip faults were distributed en échelon along the fault zone.

Inferences for the Sierras Australes

The experiment described above is not necessarily a reproduction of what occurred in the Sierras Australes. One reason for this is that the experiment made use of homogeneous brittle material; whereas the rocks at depth in the Sierras Australes were semi-brittle or ductile and the cover sequence was well layered. Another reason is that the ratio of wrenching to thrusting was both large and steady in the experiment; whereas it may not have been as large or as steady in nature.

Nevertheless, there are similarities between the surface pattern in the experiment (Fig. 16) and the outcrop pattern in the Sierras Australes (Fig 14). Most similar perhaps are the arcs. Both in the Sierras Australes and in the experiment, the arc is an asymmetric thrust belt. Towards the termination, the amount of thrusting decreases and the transport directions are roughly radial. Away from the termination, the arc in both nature and experiment grades into a right-lateral wrench zone. By analogy with the experiment, we infer that the uplifted block in Sierras Australes has undergone a counterclockwise rotation (probably less than 10°). Rotations of such small magnitudes are difficult if not impossible to detect paleomagnetically. Possibly they could be better constrained by restoration of a series of accurate cross-sections; but these are not yet available for Sierras Australes.

On a regional scale, we infer from the experiment that right-lateral wrenching along the strike of the Sierras Australes has dominated over thrusting (Fig. 14). We had no way of measuring stresses in the experiment. From the simple pattern of incipient strike-slip faults, we infer that stresses were nearly uniform and transpressive in the early stages of the experiment. We extend this interpretation to the Sierras Australes and attribute them to a regional state of transpressive stress. As for thrust vergence in the Sierras Australes, we attribute it, by analogy with the experiment, to motion on a pre-existing lithospheric fault, dipping steeply to the SW. The scale of the arc in the Sierras Australes suggests that the visible fault pattern is thick-skinned, that is, affects the upper crust.

CONCLUSIONS

(1) The Sierras Australes foldbelt underwent right-lateral transpressive motions during the Variscan orogeny.

(2) Basin formation and sedimentation at uppermost levels was coeval with faulting at intermediate levels and with low-grade ductile deformation at deeper levels.

(3) Partitioning of motions occurred at both regional and outcrop scales.

(4) In the mainly Precambrian granitic basement, transpressive deformation produced a network of mylonitic shear zones and faults. Dominant amongst these were high-angle reverse faults (top-to-NE) and right-lateral strike-slip faults (striking SE).

(5) In the Palaeozoic cover, transpression resulted in folds, upright or NE-verging, accompanied by cleavage, especially towards the base of the sequence.

(6) Partitioning at regional scale produced three distinct domains: a Northwestern Arc, a Southeastern Basin and a Central Belt.

(7) The Northwestern Arc is a fold-and-thrust belt. Overthrusting is to the northeast. Nevertheless, the arc is somewhat asymmetric: outcrop width and total deformation are greater towards the southeastern end. We attribute this asymmetry to a small component of counterclockwise block rotation about a vertical axis.

(8) The Southeastern Basin we interpret as a foreland basin associated with underthrusting to the southwest, dominated by a component of right-lateral wrenching along strike.

(9) The Central Belt we interpret as a zone of combined right-lateral wrenching and overthrusting, both in a N–S direction.

(10) Partitioning of motion in the Sierras Australes is similar to that observed in experiments where sandpacks are submitted to transpression.

As in the sandpacks, so in the Sierras Australes, we suspect that deformation may be simpler and less partitioned at depth. If so, the Sierras Australes may be due to oblique (right-lateral reverse) motion on a deep-seated NW-trending lithospheric fault, under a uniform state of transpressive stress.

The above conclusions, if correct, are valid only at the scale of the Sierras Australes themselves. They tell us nothing about the possibility of left-lateral domino motions at an even bigger scale, involving surrounding blocks. To check this possibility, further work needs to be done in neighbouring areas, especially the Sierras Septentrionales (Tandilia), 200 km to the northeast (Fig. 1).

Acknowledgements—Field work was done under the terms of a reciprocal international agreement between CNRS (France) and CONICET (Argentina) We are grateful to Professor A. J. Amos of the University of Buenos Aires for his encouragement. For our analysis of fault sets, M. Burkhard kindly made available his computer program, implemented at Rennes by J. Françolin. The experiment with the sandpack was done by Pascal Richard, at the Shell Research Laboratories in The Hague, The Netherlands, as part of another project organized by Dr W. T. Horsfield.

REFERENCES

Brun, J.-P. & Burg, J.-P 1982. Combined thrusting and wrenching in the Ibero-Armorican Arc: a corner effect during continental collision. *Earth Planet. Sci. Lett.* **61**, 319–332.

Buggisch, W. 1987. Stratigraphy and very low grade metamorphism of the Sierras Australes de la Provincia de Buenos Aires (Argentina) and implications in Gondwana correlation. *Zentbl. Miner Geol. Palaont.* **1**, 819–837.

Cingolani, C. A. & Deutsch, S. 1973. Ages Rubidium–Strontium des formations magmatiques de la Chaîne de La Ventana (Sierras Australes, Province de Buenos Aires, Argentine) *Annls Soc. géol. Belg* **96**, 263–274.

Coates, D. A. 1969 Stratigraphy and sedimentation of the Sauce Grande formation, Sierra de la Ventana, southern Buenos Aires Province, Argentina. *IUGS Symposium on Gondwana Stratigraphy*, Buenos Aires, 1967. UNESCO, Paris, 799–819.

Cobbold, P. R., Massabie, A. C. & Rossello, E. A. 1986 Hercynian wrenching and thrusting in the Sierras Australes foldbelt, Argentina. *Hercynica* **2**, 135–148.

Cucchi, R. J 1966. Petrofábrica del conglomerado de la Formación La Lola, Sierras Australes de la Provincia de Buenos Aires *Revta Asoc. geol Argent.* **21**, (2), 1–106

Du Toit, A. 1927. A geological comparison of South America with South Africa *Carnegie Inst. Washington, Publ.* **381**, 1–157.

Emmons, R C 1969 Strike-slip rupture patterns in sand models. *Tectonophysics* **21**, 93–134.

Furque, G. 1973. Descripción geológica de la hoja 34n, Sierra de Pillahuincó, Provincia de Buenos Aires *Boln Serv. nac. Miner Geol.* **141**

Gapais, D. 1989 Shear structures within deformed granites: mechanical and thermal indicators. *Geology* **17**, 1144–1147

Gapais, D., Fiquet, G. & Cobbold, P R. 1991. Slip system domains, 3. New insights in fault kinematics from plane-strain sandbox experiments. *Tectonophysics* **188**, 143–157.

Harrington, H. J 1947. Explicación de las hojas geológicas 33m y 34m, Sierras de Curamalal y de la Ventana, Provincia de Buenos Aires *Boln. Serv. nac. Miner. Geol.* **61**.

Harrington, H. J. 1980. Sierras Australes de la Provincia de Buenos Aires *Segundo Simposio de Geología Regional Argentina. Academia Nacional de Ciencias, Córdoba*, **II**, 967–983.

Horsfield, W. T. 1977. An experimental approach to basement-controlled faulting. In: *Fault Tectonics in N.W. Europe* (edited by Frost, R. T C. & Dikkers, A. J.). *Geologie Mijnb.* **56**, 363–370.

Janecke, S U & Evans, J P. 1988. Feldspar-influenced rock rheologies. *Geology* **16**, 1064–1066.

Japas, M. S. 1986. Caracterización geométrico-estructural del Grupo Pillahuincó. I. Perfil del Arroyo Atravesado, Sierra de las Tunas, Sierras Australes de Buenos Aires. *An. Acad Cienc. exact. fís. nat B. Aires* **38**, 145–156.

Japas, M. S. 1987. Caracterización geométrico-estructural del Grupo Pillahuincó II. Formación Sauce Grande Perfil del Cordón Mambacher y Sierra de las Tunas occidental, Sierras Australes de Buenos Aires *An. Acad Cienc exact. fís nat. B Aires* **39**, 125–144

Japas, M. S 1989. Las Sierras Australes de Buenos Aires: nuevas evidencias de un sistema de deformación en un régimen transpresivo. *Reunión Geotransectas América del Sur*, Mar del Plata, 202–207

Krantz, R. W. 1991. Measurements of friction coefficients and cohesion for faulting and fault reactivation in laboratory models using sand and sand mixtures. *Tectonophysics* **188**, 203–207

Llambías, E. J & Prozzi, C. R. 1975. Ventania. *Sexto Congreso Geológico Argentino, Relatorio*, Buenos Aires, 79–101.

Lluch, J. J 1976. Diagénesis y metamorfismo en las Sierras Australes. Unpublished manuscript.

Mitra, G. 1984. Brittle to ductile transition due to large strains along the White Rock thrust, Wind River Mountains, Wyoming. *J. Struct. Geol.* **6**, 51–61

Naylor, M A , Mandl, G & Sijpesteijn, C H K. 1986. Sandbox models of wrench faulting. *J. Struct. Geol.* **8**, 737–752.

Pfiffner, O. A. & Burkhard, M. 1987. Determination of paleo-stress axes orientations from fault, twin and earthquake data. *Annls Tectonicae* **1**, 48–57.

Reinoso, M. 1968. Paleocorrientes de la Formación Providencia, Devónico, Sierras Australes de la Provincia de Buenos Aires. *Revta Asoc. geol. Argent.* **23** (4), 287–296.

Richard, P. 1990. Champs de failles au dessus d'un décrochement de

socle: modélisation experimentale. *Mém. Documents Centre Armoricain d'Etude Structurale des Socles* **34**.

Richard, P. & Cobbold, P. R. 1989. Structures en fleur positives et décrochements crustaux: modélisation analogique et interprétation mécanique. *C. r. Acad. Sci., Paris Sér.* II, **308**, 553–560.

Sanderson, D. J. 1982. Models of strain variation in nappes and thrust sheets: a review. *Tectonophysics* **88**, 201–233.

Sanderson, D. J. & Marchini, D. 1984. Transpression. *J. Struct. Geol.* **6**, 449–458.

Sellés Martínez, J. 1989. The structure of the Sierras Australes (Buenos Aires Province, Argentina): an example of folding in a transpressive environment. *J. South Am. Earth Sci.* **2**, 317–329.

Simpson, C. 1985. Deformation of granitic rocks across the brittle-ductile transition. *J. Struct. Geol.* **7**, 503–511.

Suero, T. 1972. Compilación geológica de las Sierras Australes de la Provincia de Buenos Aires. *Ministerio de Obras Publicas, Laboratorio de Ensayo de Materiales e Investigaciones Tecnológicas (LEMIT)*, La Plata, Serie II, No. 216.

Suero, T. 1973. Perfiles geológicos de las Sierras Australes de la Provincia de Buenos Aires. *Ministerio de Obras Publicas, Laboratorio de Ensayo de Materiales e Investigaciones Tecnológicas (LEMIT)*, La Plata, Serie II, No. 236.

Van der Pluijm, B. A. 1990. Synchroneity of folding and cross-cutting cleavage in the Newfoundland Appalachians? *J. Struct. Geol.* **12**, 1073–1076.

Varela, R. & Cingolani, C. A. 1975. Nuevas edades radimétricas del basamento aflorante en el perfil del Cerro Pan de Azúcar-Cerro del Corral y consideraciones sobre la evolución geocronológica de las rocas ígneas de las Sierras Australes, Provincia de Buenos Aires. *Sexto Congreso Geológico Argentino, Actas*, Buenos Aires.

Varela, R., Leone, E. M. & Manceda, R. 1986. Estructura tectónica en la zona del Cerro del Corral, Sierras Australes de Buenos Aires. *Revta Asoc. geol. Argent.* **41**, (3, 4), 256–261.

Von Gosen, W. & Buggisch, W. 1989. Tectonic evolution of the Sierras Australes fold and thrust belt (Buenos Aires Province, Argentina)—an outline. *Zentbl. miner. Geol. Paläont.* **1**, 947–958.

Von Gosen, W., Buggisch, W. & Krumm, S. 1991. Metamorphism and deformation mechanisms in the Sierras Australes fold and thrust belt (Buenos Aires Province, Argentina). *Tectonophysics* **185**, 335–356.

White, S. H. 1976. The effects of strain on the microstructures, fabrics and deformation mechanisms in quartzites. *Phil. Trans. R. Soc. Lond.* **A283**, 69–86.

Woodcock, N. H. & Fischer, M. 1986. Strike-slip duplexes. *J. Struct. Geol.* **8**, 725–735.